

UNCLASSIFIED

AD NUMBER

AD068959

NEW LIMITATION CHANGE

TO

Approved for public release, distribution
unlimited

FROM

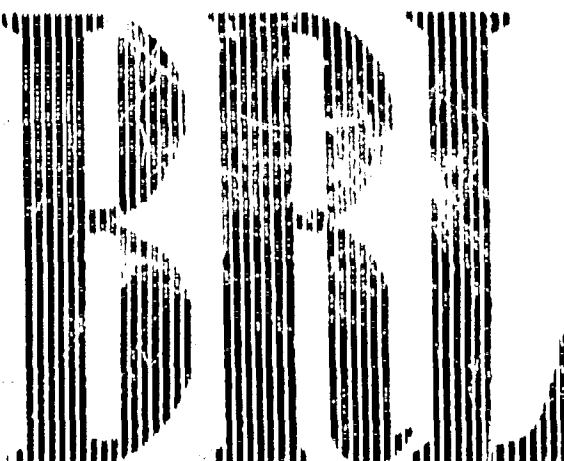
Distribution authorized to U.S. Gov't.
agencies and their contractors;
Administrative/Operational Use; MAY 1955.
Other requests shall be referred to
Ballistic Research Labs., Aberdeen Proving
Ground, MD.

AUTHORITY

BRL ltr, 22 Apr 1981

THIS PAGE IS UNCLASSIFIED

68-934
in 111.



F C

REPORT No. 934

**The Aerodynamic Properties
Of A Simple Non Rolling
Finned Cone-Cylinder
Configuration Between
Mach Numbers 1.0 And 2.5**

L. C. MacALLISTER

DEPARTMENT OF THE ARMY PROJECT No. BB03-03-001
ORDNANCE RESEARCH AND DEVELOPMENT PROJECT No. TS3-0108

BALLISTIC RESEARCH LABORATORIES



ABERDEEN PROVING GROUND, MARYLAND

BALLISTIC RESEARCH LABORATORIES

REPORT NO. 934

MAY 1955

THE AERODYNAMIC PROPERTIES OF A SIMPLE NON ROLLING FINNED
CONE-CYLINDER CONFIGURATION BETWEEN MACH NUMBERS
1.0 AND 2.5

L. C. MacAllister

Department of the Army Project No. 5B03-03-001
Ordnance Research and Development Project No. TR3-01-08

ABERDEEN PROVING GROUND, MARYLAND

TABLE OF CONTENTS

	PAGE NO.
CONTENTS	2
ABSTRACT	3
SYMBOLS	4
INTRODUCTION	5
TEST	6
DATA	8
REMARKS	12
FIGURES & GRAPHS	14
APPENDICES	31

BALLISTIC RESEARCH LABORATORIES

REPORT NO. 934

LCMacAllister/nsw
Aberdeen Proving Ground, Md.
May 1955

THE AERODYNAMIC PROPERTIES OF A SIMPLE NON ROLLING FINNED
CONE-CYLINDER CONFIGURATION BETWEEN MACH NUMBERS
1.0 AND 2.5

ABSTRACT

The aerodynamic properties of a finned model are given for a Mach number range from 1 to 2.5. The test vehicle is a ten-caliber long cone-cylinder body with four rectangular fins, of 6% thick wedge sections, set in a cruciform configuration. The data were determined by firings in a spark photography range.

SYMBOLS

<i>A</i>	- Axial moment of inertia
<i>B</i>	- Transverse moment of inertia
<i>M</i>	- Mach number
<i>S</i>	- Reference Area ($\frac{\pi d^2}{4}$)
<i>v</i>	- Velocity
<i>b</i>	- Fin span
<i>c</i>	- Fin chord
<i>d</i>	- Model diameter (caliber)
<i>k₁²</i>	- Axial radius of gyration (calibers ²)
<i>k₂²</i>	- Transverse radius of gyration (calibers ²)
<i>m</i>	- Mass
<i>q</i>	- Transverse angular velocity
\bar{q}	- Dynamic pressure, $\frac{\rho v^2}{2}$
<i>a</i>	- Angle of yaw
<i>s²</i>	- Mean squared yaw
<i>p</i>	- Air density

COEFFICIENTS (angular units-radian)

<i>C_D</i>	= Drag/ $\bar{q} S$
<i>C_{N_a}</i>	= Normal force/ $\bar{q} S a$
<i>C_{H_a}</i>	= Damping force/ $\bar{q} S (\frac{dc}{2\dot{v}})$
<i>C_{D_a}</i>	= Damping force/ $\bar{q} S (\frac{dc}{2\dot{v}})$
<i>C_{M_a}</i>	= Yaw moment/ $\bar{q} S a$
<i>C_{H_q}</i>	= Damping moment/ $\bar{q} S (\frac{dc}{2\dot{v}})$
<i>C_{D_q}</i>	= Damping moment/ $\bar{q} S (\frac{dc}{2\dot{v}})$

INTRODUCTION

Free flight range testing provides a means of obtaining the static and dynamic properties of projectiles. Historically it has been one of the most accurate means of determining the total drag of spin or fin-stabilized projectiles in supersonic flight. Free flight testing may also be necessary to determine the static force and moment properties near sonic speeds although these properties can usually be adequately determined at supersonic and subsonic speeds by other means. In the case of the dynamic forces and moments acting on the projectile only free flight testing and some special wind tunnel instrumentations are available to yield the desired information.

The Free Flight Aerodynamics Range and the Transonic Range (1, 2) of the Exterior Ballistics Laboratory are instruments for determining data to yield the aerodynamic characteristics of models or full scale missiles. The properties of several classes of bodies of revolution have been investigated (2, 4, 5, 6) and also some of the characteristics of finned shell.

An overall investigation of the motions of winged and finned projectiles of a simple type seemed advisable. The current report is concerned with one phase of the larger program: the performance of a finned projectile as a function of Mach number. Investigations of the axial (7) and the rolling motions (8, 9) of this model have already been reported as has an initial study of the model with slight asymmetry (10).

It appeared that the determination of static and dynamic characteristics, through utilization of the ranges, could be accomplished best by a study of the angular motion¹ of a symmetric, non-rolling model. Accordingly, a series of models was designed and produced to have as little net deflection of the fin surfaces as was practical. The data obtained from these cone-cylinder models with tail fins for a Mach number range of 1 to 2.5 are presented and some of the problems encountered in analyzing the observed motions discussed.

¹ Aerodynamically this motion is resolved in two components: pitch, vertically, and yaw, laterally. In ballistics the vector sum of the components is termed the yaw. The term pitch will usually be used here to denote the more general ballistic yawing motion for these models since they are predominately pitching motions in the aerodynamic sense.

TEST

The Aerodynamics Range

The Range (Fig. 1) is an enclosed firing gallery containing 46 individual spark shadowgraph stations which record horizontal and vertical projections of the missile as it passes through them. The time of flight is recorded on chronograph counters.

The model is fired from a gun through a blast chamber into the range gallery. In passing through the blast chamber the missile passes between electrostatically charged plates and acquires a triggering charge. As the charged model approaches each station (Fig. 2) an antenna loop before the station generates a signal which is amplified and delayed to permit the model to come to the center of the station before the station fires. The model is shadowgraphed in two planes and the characteristic survey marks of the station imprinted on the photographic plates. These plates yield the basic data to determine the instantaneous spatial coordinates of the missile and its angular orientation; they also provide a graphic view of the flow field about the model.

Program

The firing program was carried out in two phases. The first phase consisted of the launching of twelve models, four each of three center of mass positions. The models with various mass center positions would provide checks, through the c.m. transformations¹ (12), for consistency of the data and give a determination of the lift and damping forces. The basic Mach number was 1.8.

The second phase involved the launching of eighteen models of two center of mass positions in a range of Mach numbers from about 1 to 3.

The model configuration was ten-calibers long with a 10° semi-angle conical nose. The cruciform tail section was located at the base of the body and consisted of 8% thick wedge-airfoil sections with a one-caliber chord and an overall span of three calibers (Fig. 3).

The models were launched from a special smooth bore gun with an "X" shape bore (Figs. 4 and 5). The model was accompanied by a sabot and obturating wafers to permit launching (Figs. 3 and 5).

Some special reductions of the rounds, and also of computed motions were carried out to assess the various reduction procedures which might be applied to the motion of models of this type and to evaluate the effects of minor variations from the ideal symmetric design. These problems were suggested by earlier programs and by current work on the present program. The mechanics of, and many of the suggestions for,

¹ Appendix A

this latter work were done by members of the Data Reduction Section and only the results are discussed.¹

It is a basic requirement of the free flight range technique that in order to study the aerodynamic properties, other than drag, the model must yaw. At the inception of the first test phase, one of the more promising methods of inducing yaw with the rail gun was by means of throwers installed in the "rail extension" (Fig. 4). These devices intercept the following sabot as it clears the muzzle .cc of the extension and deflect it to the side. If at this moment the sabot is in contact with the model, some of the energy of the thrown sabot will be delivered to the model. Since this force is delivered at the model base it should result in the model:

- a. yawing away from the direction of the thrown sabot,
- b. attaining, as a result of a., an aerodynamic jump away from the sabot,
- c. acquiring some directly transmitted lateral velocity in the direction of the thrown sabot.

The latter two factors tend to nullify each other, and could conceivably permit the production of reasonable yawing motions without prohibitive lateral deflections of the model.

A preliminary program was fired to test the feasibility of this method for the present program. The results indicated that if the amount of energy transferred from the sabot to the model could be limited by, say, a fragile shear pin between the sabot and the model, the system could produce desirable yaws. It also indicated a marked sensitivity to minor variations in pin manufacture.

A general survey of the firings is given in Table II. It appears that the sabot throwers, coupled with a shear pin, can produce yaw but the system is very sensitive to several variables.² Only one model had insufficient yaw to yield a reduction but, also, only about a third of the models were at or near the most desirable yaw level.

A potentially better method was available for the second phase of the program. This method consisted of enclosing a high strength magnet in the model and launching it through the field of a powerful electromagnet. Since these firings constituted the first test of a system of

I Appendix B

² Primary errors these were: (a) variations in pin strength (after the large amount of machining necessary to reduce them to the desired shear area) (b) probable variations in the separation of the model and sabot at the instant of contact with the throwers.

this nature some difficulties were encountered that could be avoided in future firings utilizing this system.¹

The models contained four inch long, half inch diameter, Alnico V magnets and were launched through an aircooled electromagnet with a maximum field strength of 18,000 Gauss² (Fig. 6). In the main it provided a reliable source of yaw.

Table I gives the physical properties of the models and Table II the launching conditions.

AERODINAMIC DATA

General Treatment

The range data were processed by the usual reduction techniques applied to spinning shell and by special reduction techniques set up for this program (12). The test data of the first group were obtained in a Mach number region of $1.73 \leq M \leq 1.84$ and at an average yaw level up to eight degrees. Primarily these models furnished a check of the variation of the aerodynamic properties with center of mass position for one Mach number and secondarily the variation of some of the coefficients with yaw level.

The second group was fired from $0.98 \leq M \leq 2.5$ and with average yaws up to four degrees. These models furnished data primarily as functions of Mach number. Only in the case of the drag coefficient were correlations with yaw level practical.

Drag

The drag coefficient, C_D , is given in Table III and in Graphs I and II as a function of Mach number and yaw.

The value of the drag coefficient descends fairly sharply from a peak at about $M = 1.05$ until Mach number 1.3 and thereafter decreases more slowly with increasing Mach number. The portion of the curve near sonic velocity is not as well determined as the remainder since there is only one data point below $M = 1$.

The yaw drag coefficient decreases from about 15.0 per radian squared to 8.9 from a Mach number of 1.4 to 2.4.

¹ Primarily strong there was the extreme variability in resistance to demagnetisation among the first lot of magnets procured. Later lots appear to be free of this defect.

² The theory of the Electromagnetic Yaw Inducer and the detailed results will be the subject of another report and will not be considered here.

Several models of the second group had stable laminar boundary layers over the cone and part of the cylindrical body. Since the majority of the models had turbulent layers over the whole body, the frictional drags of the models with laminar layers were corrected to a full turbulent condition and the curve drawn for this latter state.

Yaw Moment and Center of Pressure

The yaw moment derivative, C_M , is given in Table III, in Graph IV as a function of Mach number, and in Graph V as a function of center of mass position for $M = 1.8$. The movement of the center of pressure of the normal force as a function of Mach number is presented in Graph III.

The behavior of the moment coefficient appears typical above $M = 1.4$. A minimum value for the two center of mass positions occurs near a Mach number of 1.2. Below this speed the value of C_M increases slightly to a maximum value between $M = 1.05$ and 1 and appears to decrease sharply subsonically (although this latter behavior hinges on one point below $M = 1$).

The phase I tests indicated a linear variation with center of mass positions for the three c.g. positions used at $M = 1.8$. The slope of the curve (Graph V) yields C_N for this Mach number.

The center of pressure appears to be in a maximum rearward position near $M = 1$ at about 1-1/4 calibers from the base and moves forward for greater or lesser speeds. As Mach number increases the c.p. moves forward until about $M = 1.1$, rearward until $M = 1.4$ and there begins to move forward again steadily with increasing Mach number. A position of about 2.6 calibers forward of the base would be reached by $M = 2.6$.

Normal Force

The normal force coefficient could be determined by two methods in this program. The variation of the yaw moment as a function of center of mass position at a given Mach number determines the derivative of the normal force via the c.m. transformation.¹ The transverse motion of the center of mass of the projectile in response to the lift force can also be used to determine the lift (hence normal) force through an analysis of the swerving motion. Both methods have advantages and disadvantages. On the credit side the c.m. transformations involve only physical dimensions and the well determined moment coefficients. However, two separate rounds are involved which cannot be exactly the same shape. In addition, interpolation of the moment values with respect to Mach number is usually required to determine the normal force at a given Mach number. The lift coefficient is obtained from an individual round through the swerve reduction. However, this reduction is

¹ Appendix B

subject to adverse conditions: (1) the actual displacement involved is small, on the order of a tenth of an inch; (2) the swerve equations rely on the accuracy of the yaw determination, and since this involves a double integration of the yaw the swerve fitting is very sensitive to even minor anomalies in the yawing motion. Both methods were used and are shown in Graph VI.

The normal force coefficient, C_{N_a} , appears to follow, qualitatively, the trend of the moment coefficient. At about $M = 1.1$ a minimum C_{N_a} of about - 25 is reached and the value then increases to about - 14.9 at $M = 1$. It appears to decrease for the lower speed.

Damping Moment

The damping moment derivatives, $(C_{M_q} + C_{M_a})$ are determined from the total damping of the yawing motion once the lift force derivative and the drag coefficient are known. Hence the accuracy of the determination of these coefficients hinges on the overall fitting accuracy of the yawing motion and the accuracy of the determination of the lift coefficient C_{L_a} .

The damping moment derivatives are a quadratic function of center of mass position. This variation is given in Graph VII for the first group of models ($M = 1.8$). The least damping occurs for a c.m. position 2.1 calibers from the base.

$(C_{M_q} + C_{M_a})$ values are given for two center of mass positions as a function of Mach number in Graph VIII. The overall behavior is similar for both c.m. positions. The value increases from a large negative level near $M = 1$ to an ill-defined and possibly positive value at about $M = 1.05$ and thereafter decreases rapidly to a maximum negative value at $M = 1.3$. At higher Mach numbers there is a general tendency to decrease in magnitude.

Damping Forces

The damping force coefficients, $(C_{N_q} + C_{N_a})$ can be determined by two methods, in manners analogous to those used to determine the lift coefficient. $(C_{N_q} + C_{N_a})$ can be isolated by a comparison of the

damping¹ moments from models with two c.m. positions or from the swerve of the individual model due to the damping forces.

The accuracy with which the damping moments are determined is lower than that of the yaw moment, hence the damping force determination from two moments is weaker than the similar process for the lift. In the cases of determination from the swerving motion it should be noted that the displacement due to the damping forces is considerably less than the displacement due to lift. In view of this it is gratifying that the better determined values from the swerve are in reasonable agreement with the curve determined from the damping moment.

$(C_{N_q} + C_{N_a})$, evaluated at the centroid, is given in Graph IX as a function of Mach number.

Observable Phenomena and Variation of the Aerodynamic Properties

A series of shadowgraphs showing the flow field at different Mach numbers is given in Fig. 7 & 8. The relation of the observed drag and the state of the boundary layer has been discussed. Other properties of the changing flow pattern with Mach number also seem to be reflected in definite changes of the various force and moment properties. A correlation is given in Table IV. In general two major changes in the flow, the attachment of the body shock and the attachment of the fin shock system, appear to influence all the coefficients. The Mach numbers associated with the interaction of the fin tip Mach cone with the body and with the onset of fin-on-fin interference also appear to be points of change for some parameters.

In the case of the better determined properties, the general behavior is qualitatively explainable from consideration of the model as a sum of the properties of the body alone and the tail alone. The moment coefficient may be considered as an example.

The moment coefficient decreases with decreasing Mach number from $M = 2.5$ to 1.4 in a manner suggesting the theoretical variation of wing lift with Mach number. The value continues to decrease until $M = 1.15$ but with a decreasing rate as the three dimensional tip effects influence more and more the neighboring surfaces. At $M = 1.15$ the fin shock system detaches and the tail suffers a loss of lift.

¹ As noted in Appendix A the variation of the damping moment coefficients is a quadratic function of center of mass position and involves C_{N_a} , C_{M_a} , and $(C_{N_q} + C_{N_a})$. This complicates the determination of the latter coefficients. However, a function of $(C_{N_q} + C_{N_a})$ and C_{M_a} can be constructed so that the function varies linearly with c.m. with a slope directly related to $(C_{N_q} + C_{N_a})$.

The body, however, is still supersonic and its destabilizing moment is still increasing with decreasing Mach number. Hence the moment coefficient increases from $M = 1.15$ until $M = 1.05$ when the body shock detaches and equalizes matters. Below $M = 1.05$ the moment decreases in magnitude.

REMARKS

The use of models designed, and carefully manufactured, to produce a pure pitching motion in the firing range is a feasible method for determining the static and dynamic aerodynamic properties of a finned missile. Actually however, a considerable number of the projectiles so manufactured will not be perfect enough and will exhibit a rolling motion and/or trimmed flight. In order to yield the best data these models must be treated by reductions that permit roll and asymmetry, or must be discarded. As is noted in the Appendix B these defects introduce errors in the determinations of the yaw damping and of the lift and damping force from the swerving motion if only symmetric reductions and/or non-rolling reductions are used.

In the present program practical accuracy could have been obtained by symmetric-non-rolling reductions on all but two rounds as long as it was not necessary to rely on the fit of the swerving motion to determine the lift. Approximately a third of the models required asymmetric reductions to yield good lift coefficients from the swerve.

L C MacAllister
L. C. MacAllister

REFERENCES

1. Rogers, W.R., The Transonic Free Flight Range, BRL 849.
2. Charters, A.C., Some Ballistic Contributions to Aerodynamics, JAS, Vol. 14, No. 3, 1947.
3. Murphy, C.H., Schmidt, L.E., Effect of Length on the Aerodynamic Characteristics of Bodies of Revolution in Supersonic Flight, BRL 876 (C).
4. Murphy, C.H., Schmidt, L.E., The Aerodynamic Properties of the 7-Caliber AN Spinner Rocket in Transonic Flight, BRLM 775.
5. Schmidt, L.E., The Dynamic Properties of Pure Cones and Cone-Cylinders, BRLM 759.
6. Charters, A.C., Thomas, The Aerodynamic Performance of Small Spheres from Subsonic to Supersonic Flight, JAS, Vol. 12, No. 4, 1945.
7. MacAllister, L.C., The Drag of Long Arrow Projectiles, BRLM 600.
8. Nicolaides, J.D., Boltz, R.E., The Determination of Some Aerodynamic Coefficients from Supersonic Free Flight Tests of a Rolling Missile, BRL 711.
9. Nicolaides, J.D., Boltz, R.E., On the Pure Rolling Motion of Winged and/or Finned Missiles in Varying Supersonic Flight, BRL 799.
10. Nicolaides, J.D., On the Free Flight Motions of Projectiles with Slight Configurational Asymmetry, BRL 858.
11. Kelly, McShane, Reno, Exterior Ballistics, Denver Press, 1953.
12. Murphy, C.H., Data Reduction for the Free Flight Spark Ranges, BRL 900.
13. Nicolaides, J.D., Variation of the Aerodynamic Force and Moment Coefficients with Reference System, BRL TN 746, 1952.
14. Murphy, C.H., On the Stability Criteria of the Kelly-McShane Linearized Theory of Yawing Motion, BRL 853.



FIG. 1. Free Flight Aerodynamics Range.

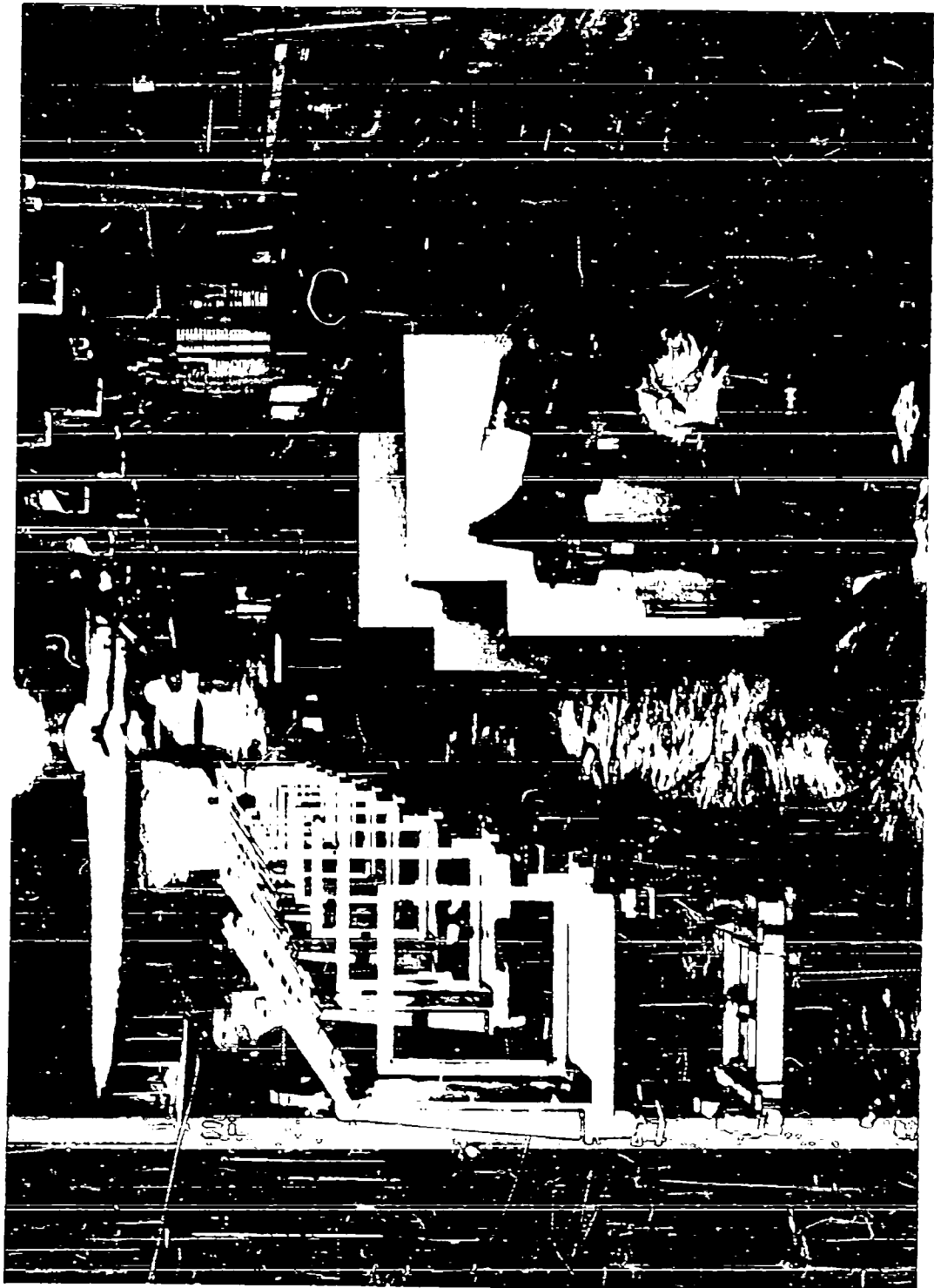


FIG. 2. View of Range Station.

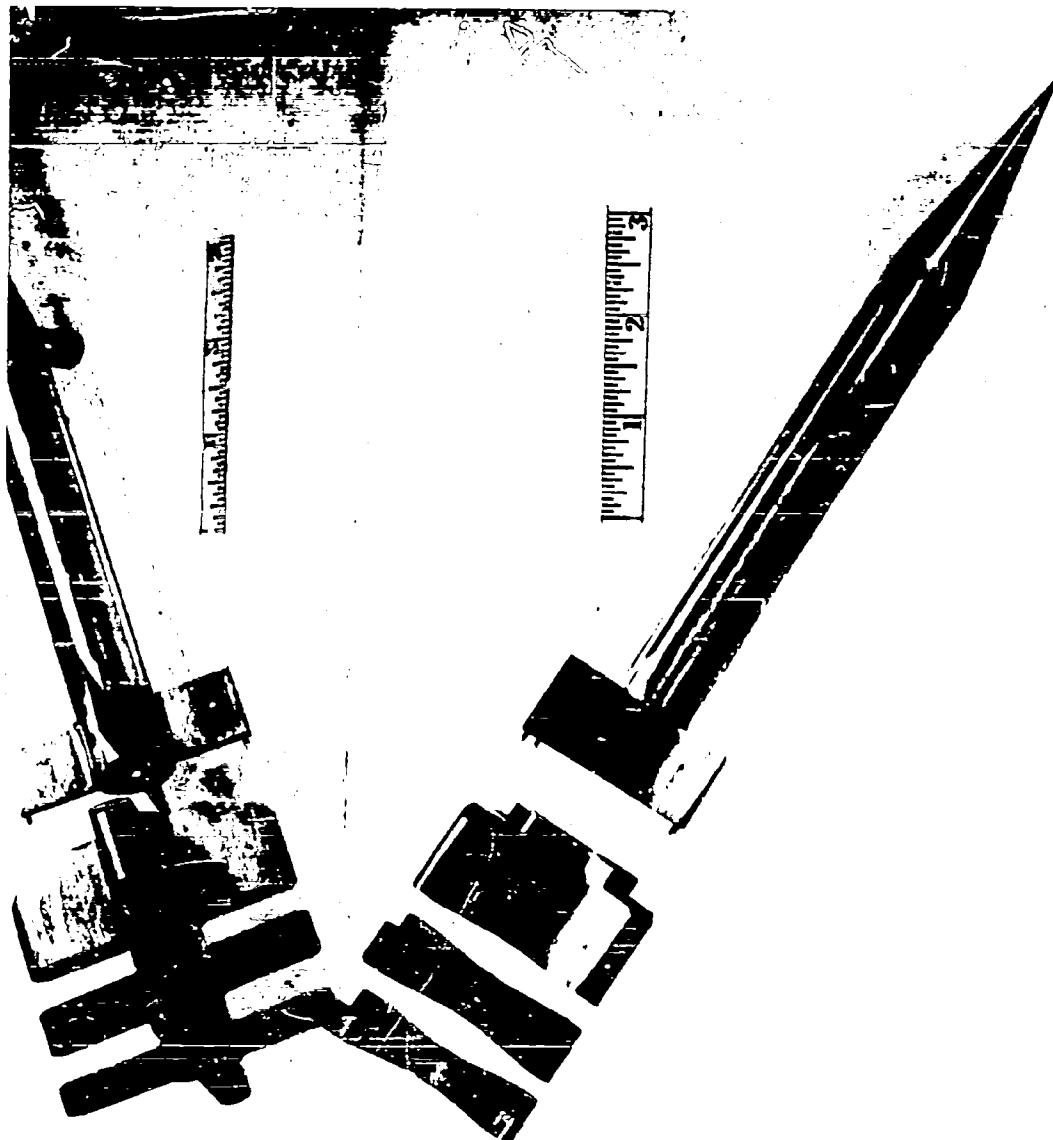


FIG. 3. Model with Sabot and Seating Disk.



FIG. 4. Muzzle View of Rail Gun.

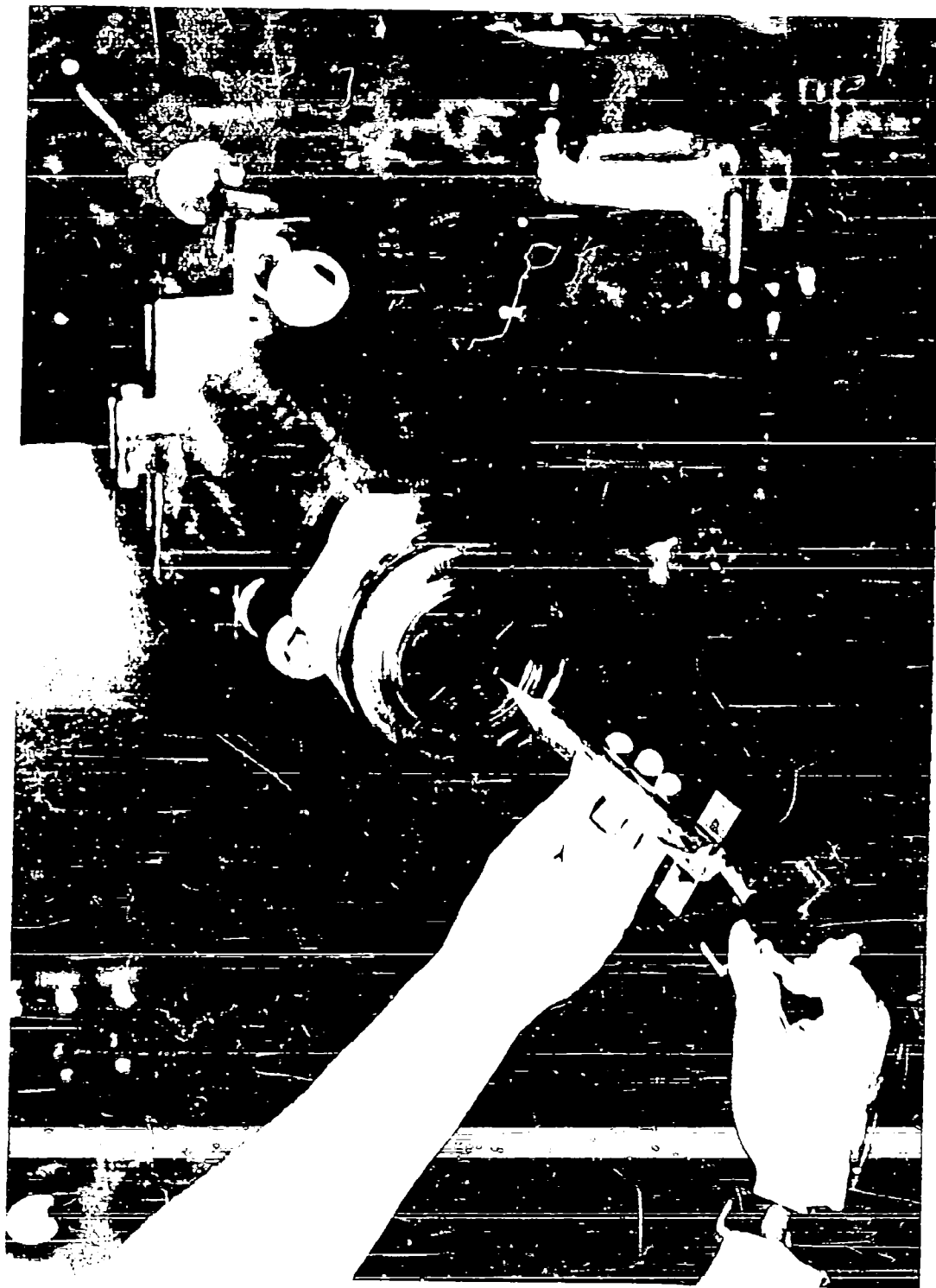
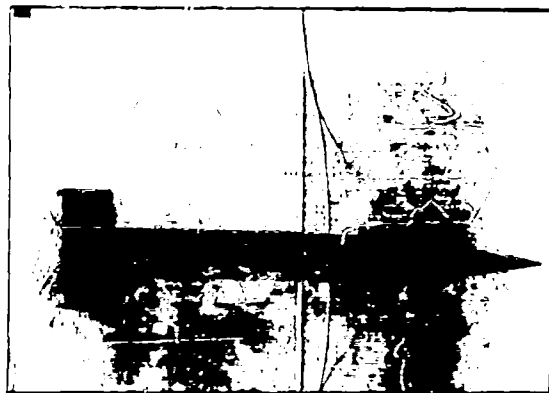


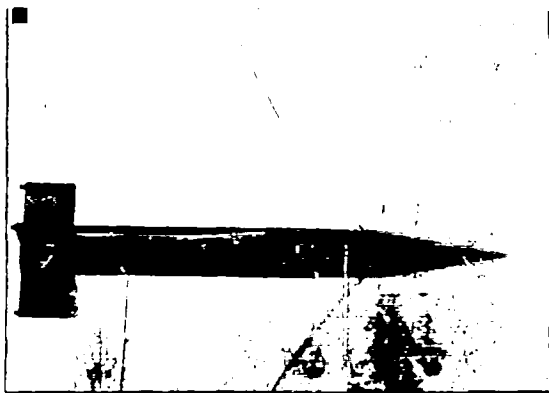
FIG. 5. Breech of Rail Gun With Model Being Loaded.



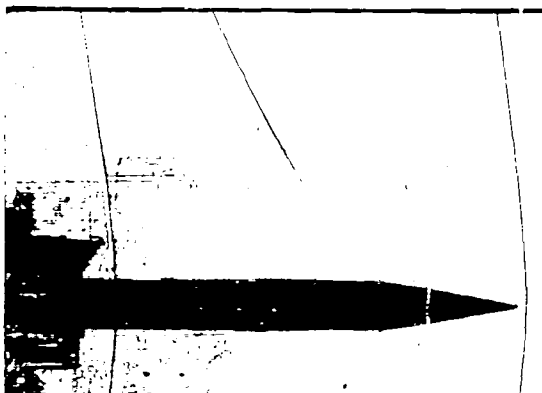
FIG. 6. Electro-Magnetic Yaw Inducer.



$M = 0.975$



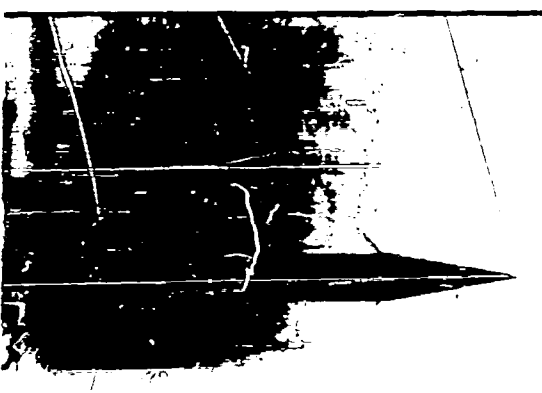
$M = 1.016$



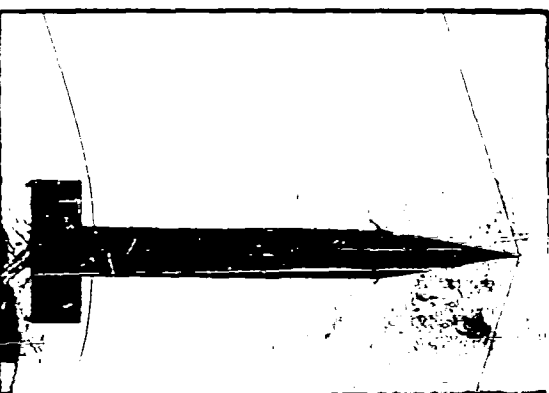
$M = 1.034$



$M = 1.058$

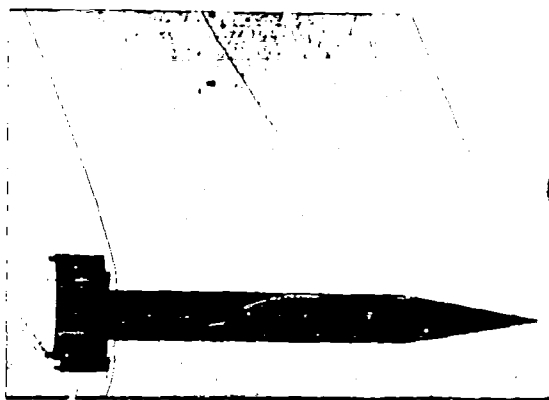


$M = 1.063$

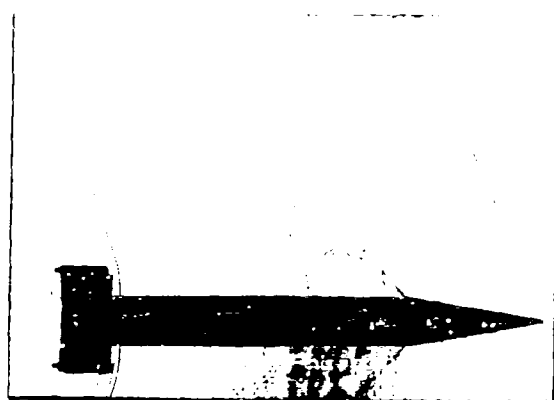


$M = 1.070$

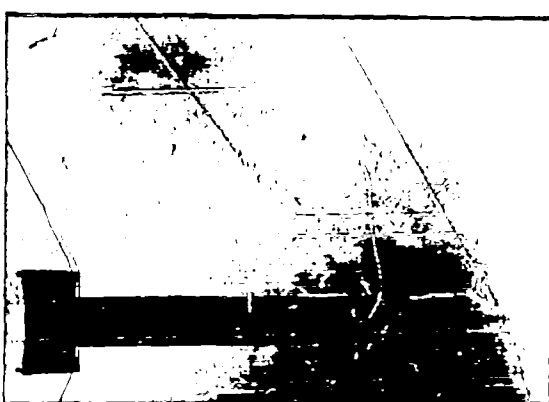
FIG. 7. Flow Shadowgraphs.



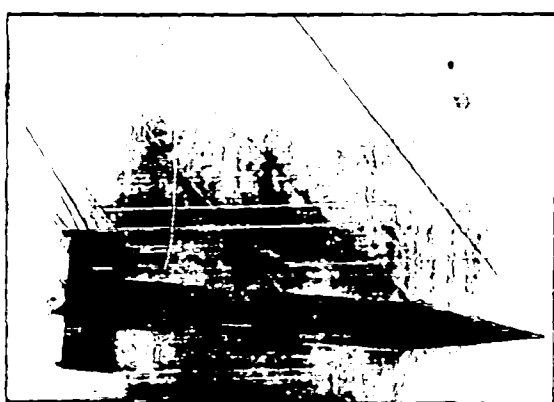
M = 1.10



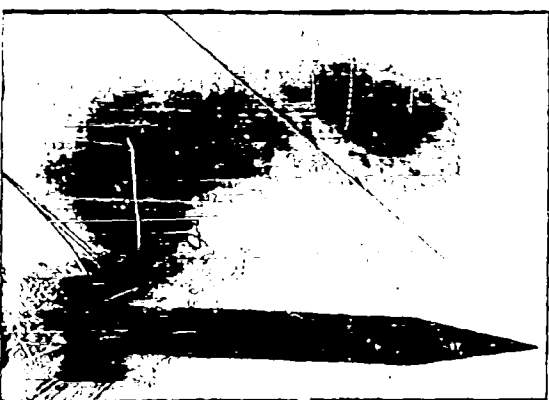
M = 1.12



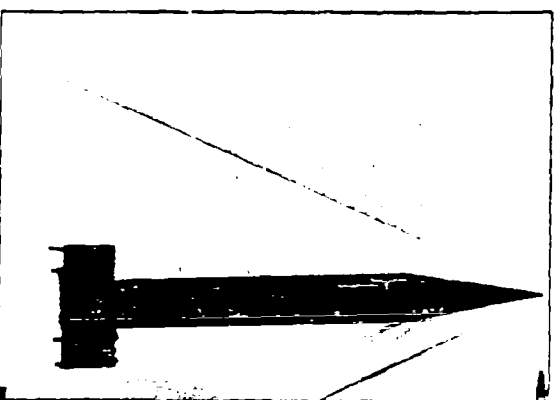
M = 1.16



M = 1.28

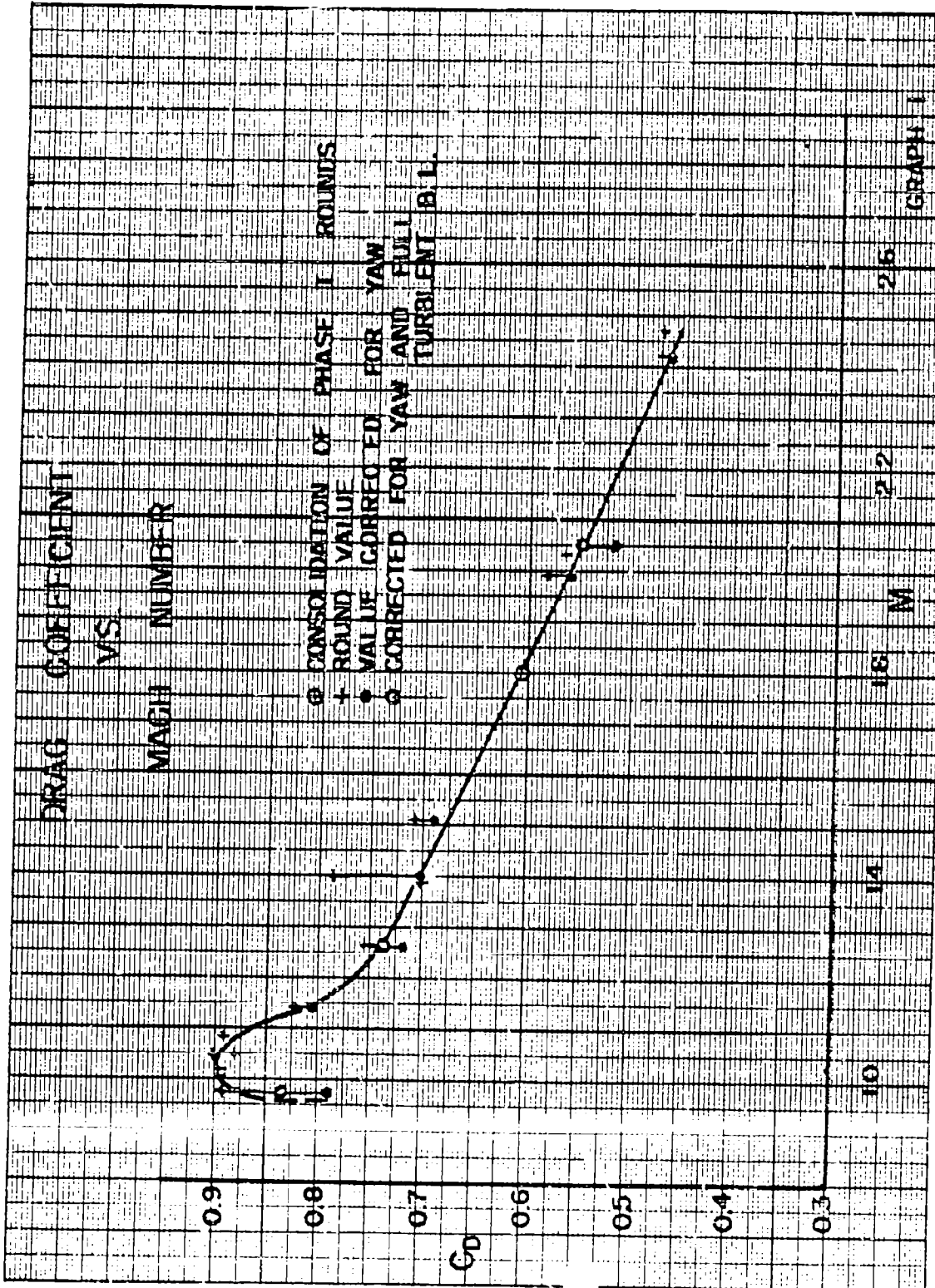


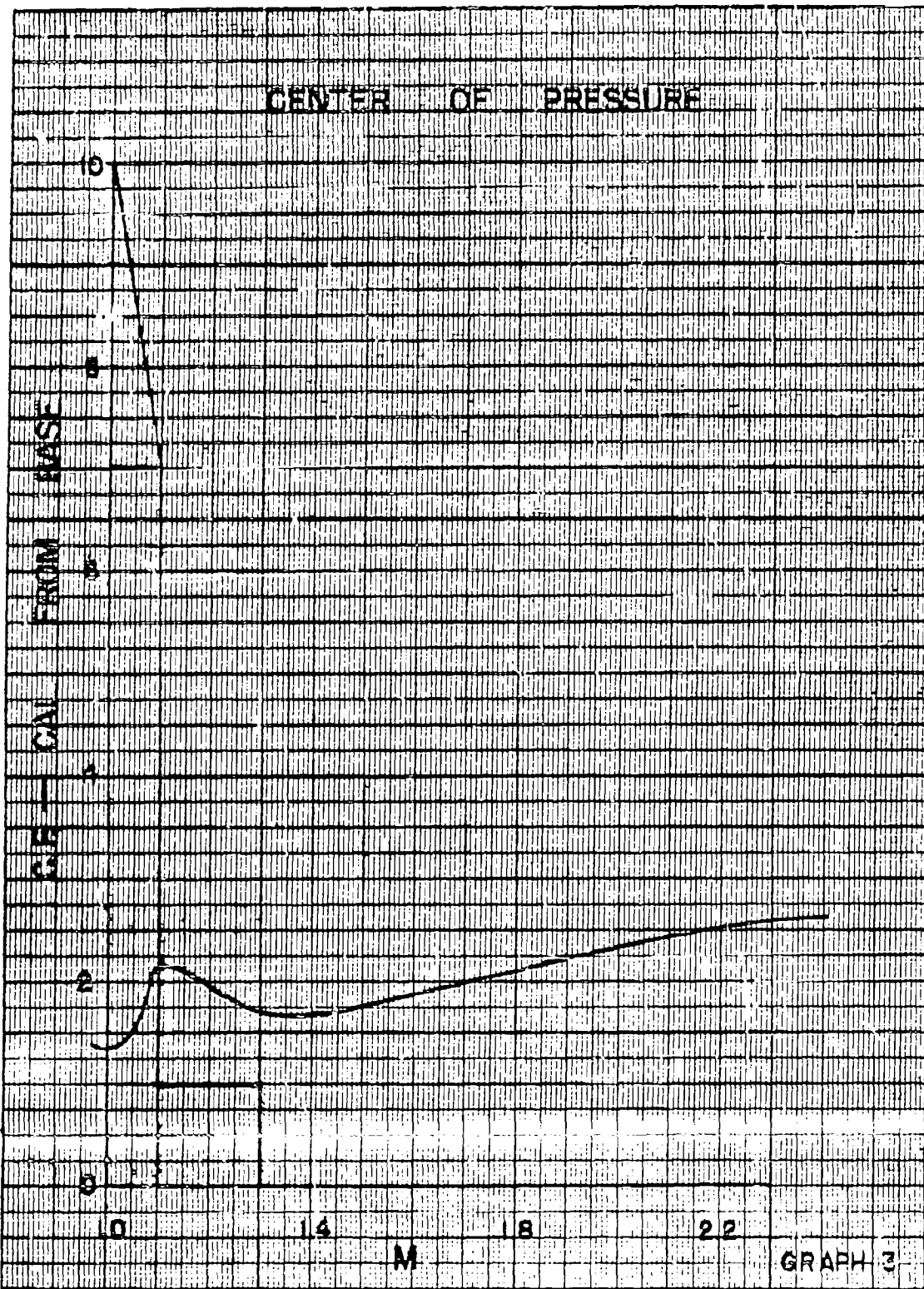
M = 1.53

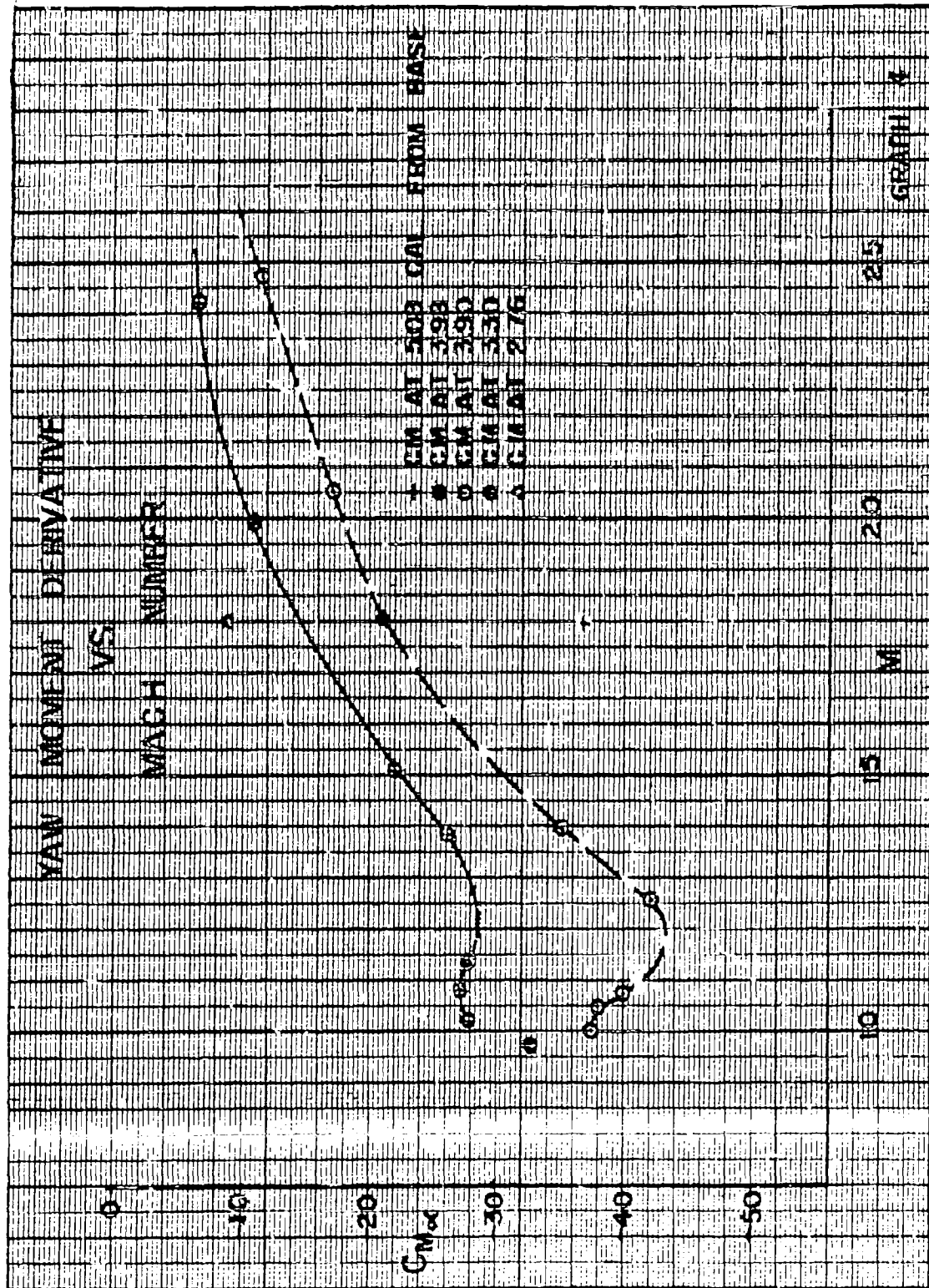


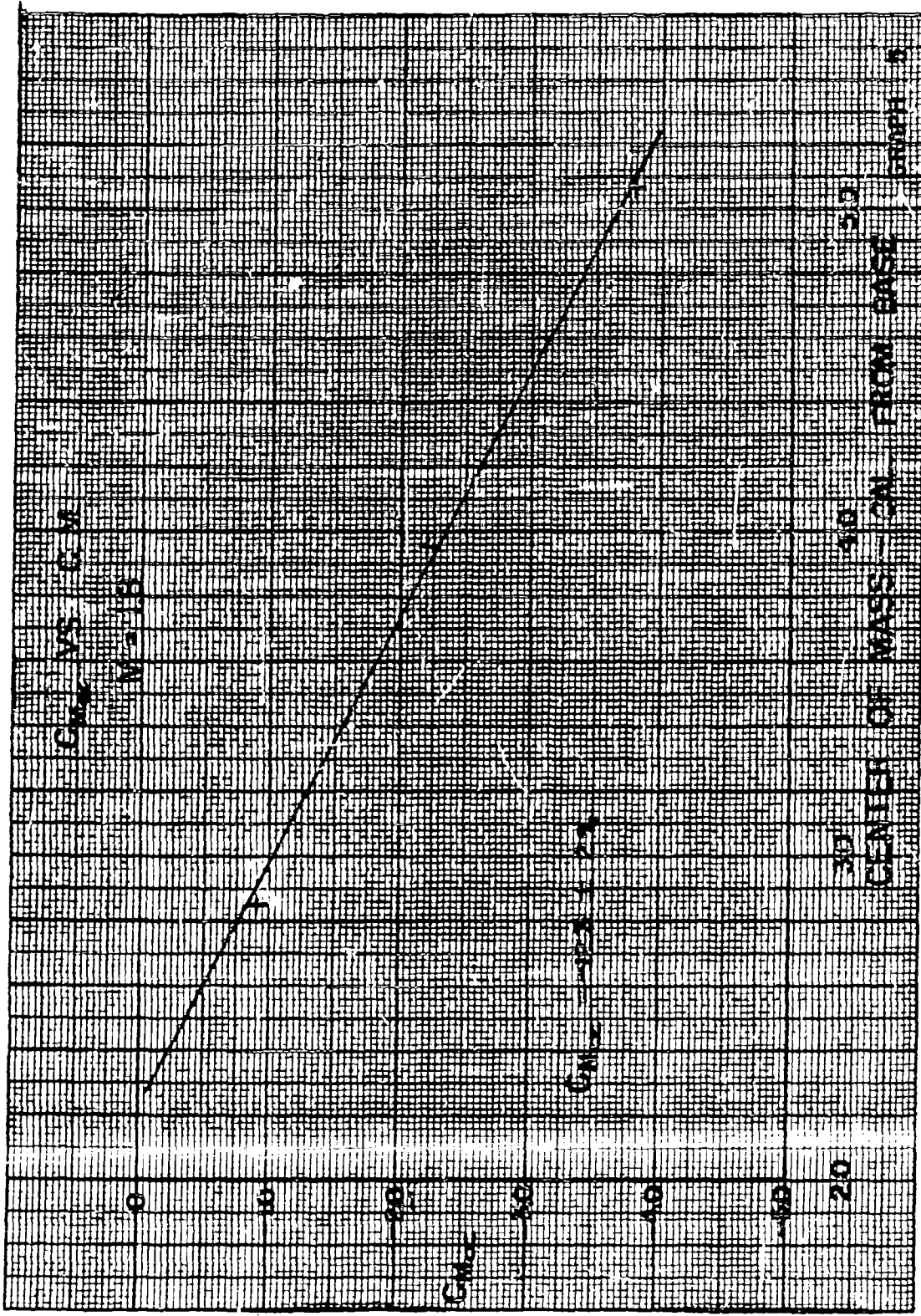
M = 2.51

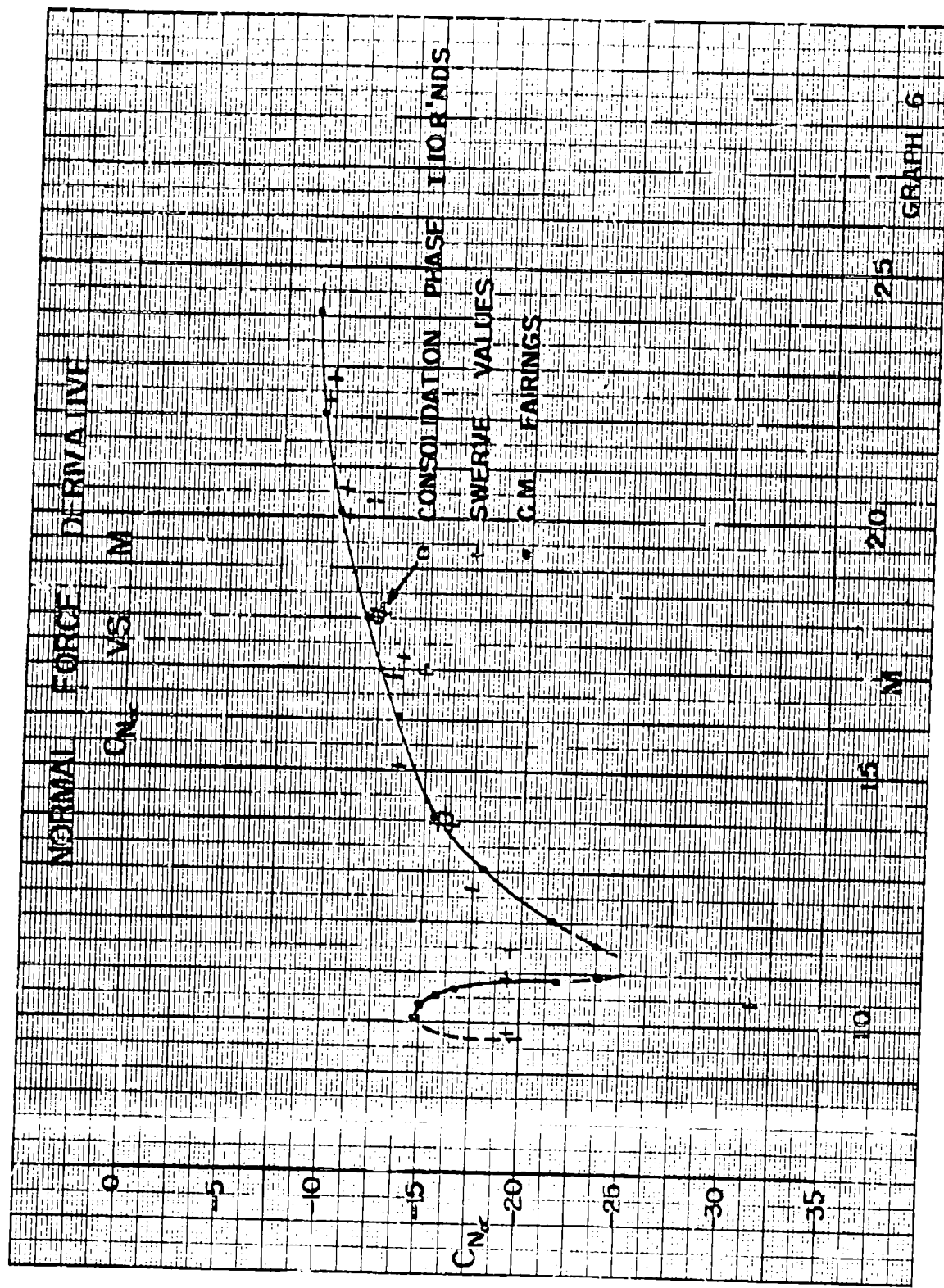
FIG. 8. Flow Shadowgraphs.

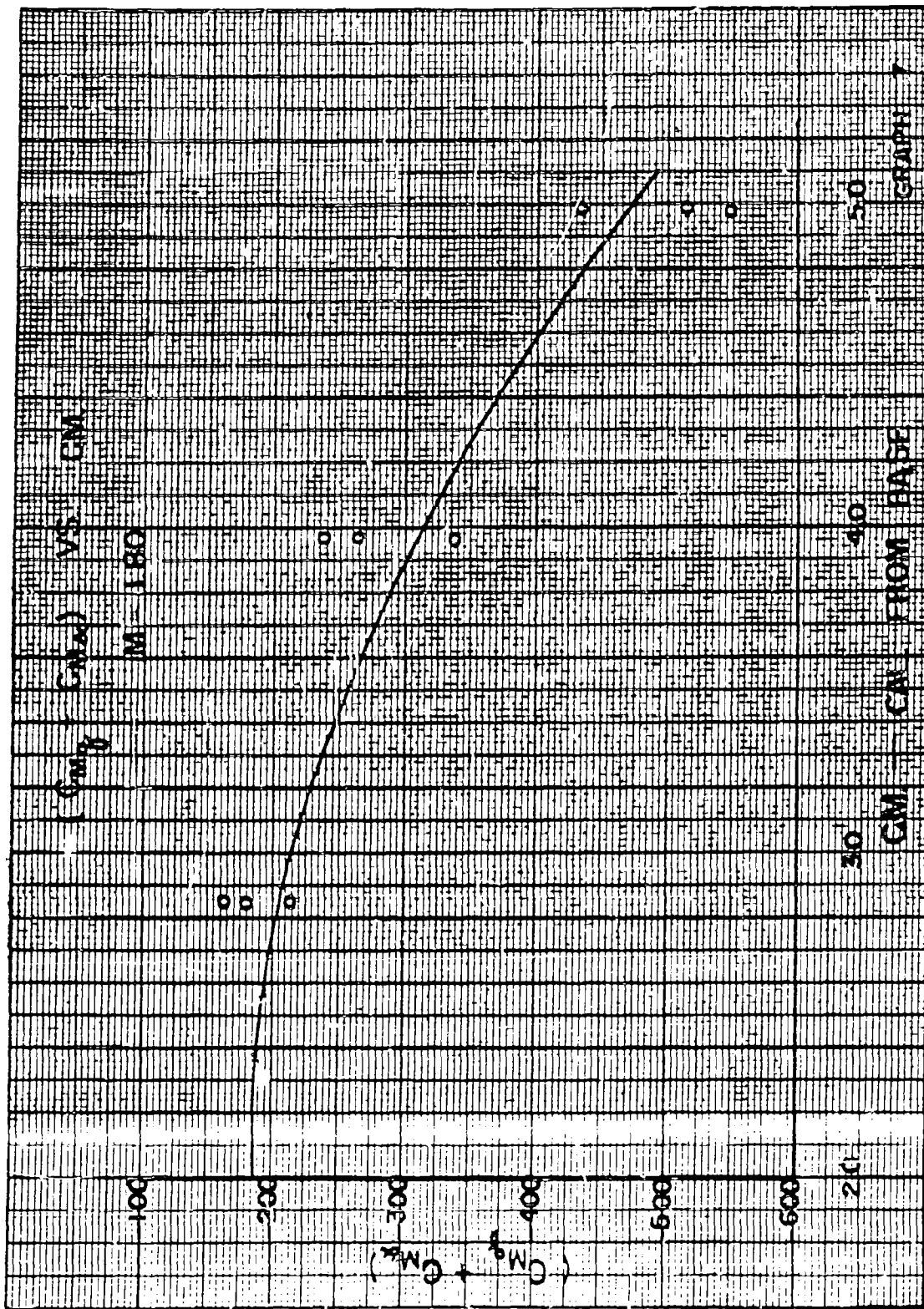


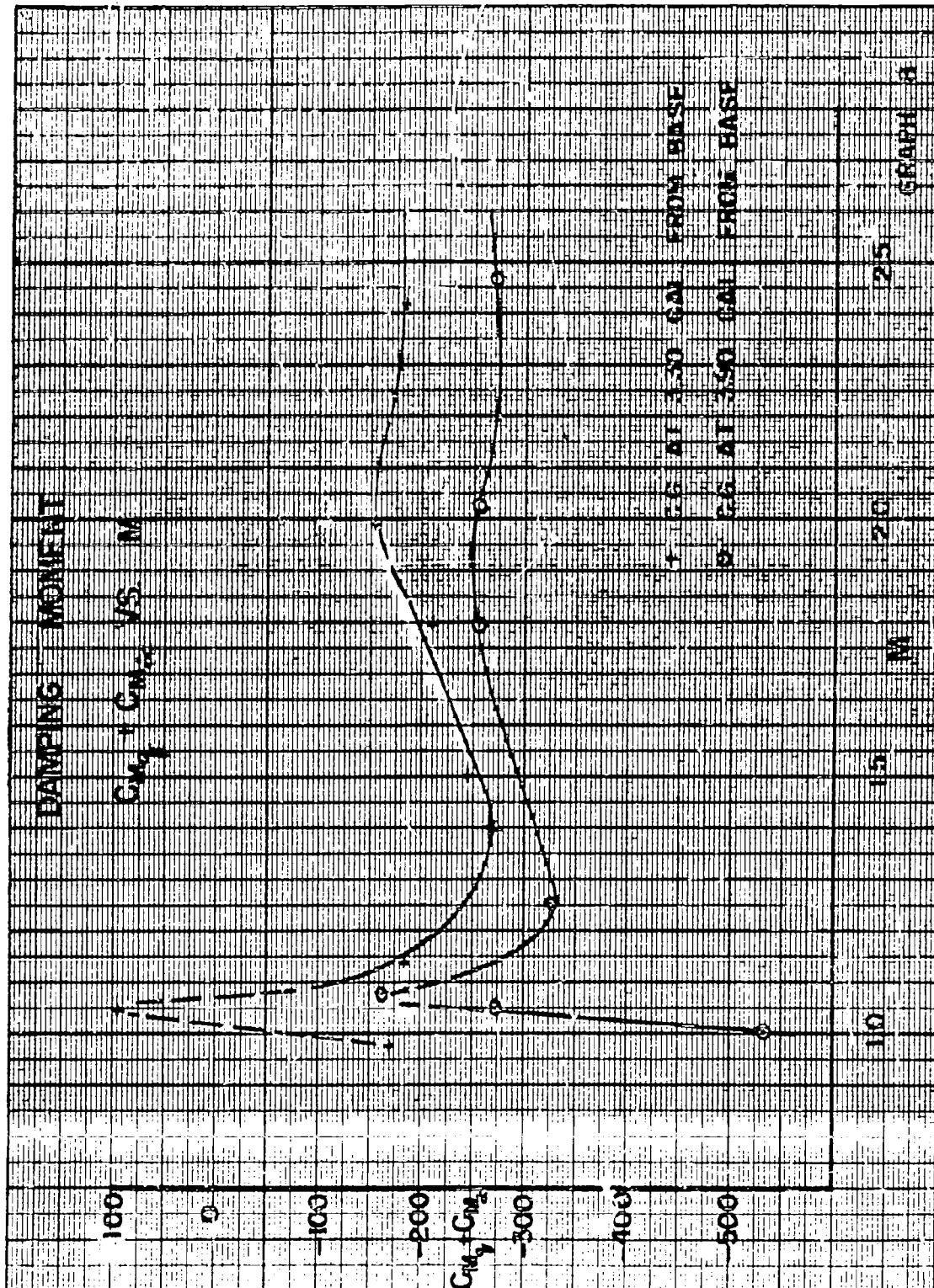


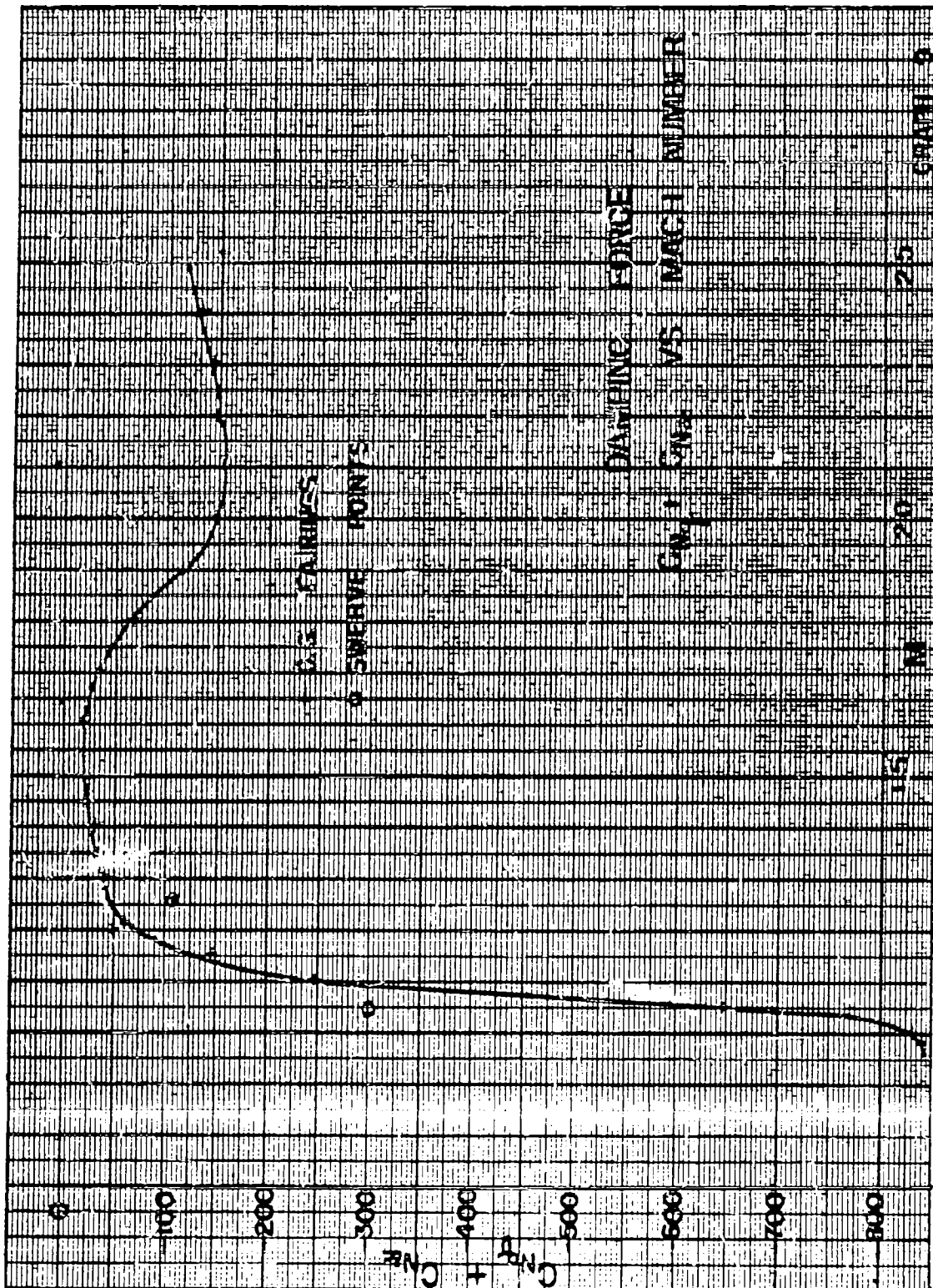












APPENDIX A

Fitting Equations and Transformations

The equations utilized in processing firing range data are repeated here for convenience. Further details may be obtained from the indicated references.

Firing Motions

The equation¹ usually used for fitting the observed motion of spinning shell is⁽¹²⁾

$$(1) \lambda = \sum_{j=0}^2 K_{j0} e^{-\alpha_j p + i(\beta_{j0} + \beta'_{j0}p + \beta''_{j0}\frac{p^2}{2})}$$

where p is distance along the trajectory in calibers. K_{j0} and β_{j0} are initial constants. The aerodynamic parameters are related to the fitting parameters as follows:

$$(2) k_2^{-2} c_{M_a} (\frac{\rho S_0}{2m}) = \beta'_1 \cdot \beta'_2 - a_1 a_2 + \frac{\epsilon_1}{2} \hat{D} (a_1 + a_2 - \frac{\epsilon_1}{2} \hat{D})$$

$$\therefore \beta'_1 \cdot \beta'_2 = a_1 a_2^2 \text{ (footnote)}$$

and

$$(3) \frac{pd^3}{m} \left[-c_{M_a} \left(\frac{d}{2d^2} \right) - 2c_D \left(\frac{S}{2d^2} \right) - k_1^{-2} (c_{M_a} + c_{M_d}) \frac{S_0^2}{4d^4} \right] = (a_1 + a_2) - \hat{D} \epsilon_1^2 \text{ (footnote)}$$

and generally with spinning shell¹

$$(4) \frac{\beta'_1 + \beta'_2}{\beta'_1 \cdot \beta'_2} = \frac{v^2}{V^2} \cdot \hat{D}^2$$

-
- ¹ Reduction Symbols: $\lambda =$ Complex yaw $\lambda_x + i\lambda_y$
 $S =$ Swerve, $x + iy$, motion transverse to the mean trajectory
 $\beta'_1 =$ Epicyclic turning rates
 $a_1 =$ Epicyclic damping rates
 $()' = \frac{d()}{dp}$

- ² Normally $\hat{D} = J_\Sigma - k_1^{-2} J_A (1 - \frac{1}{V})$ in terms of the ballistic J factors and $\epsilon_1 \sim v$, the spin in radians per caliber. Hence this term should be zero or very small for the present case.

Equation (1) involves 10 unknowns, K_{j0} , θ_{j0} , a_j , θ'_{j0} , and θ''_{j0} for $j = 1, 2$. It can be shown that if the spin is zero and Mach number variation is negligible for the observed flight that it is possible to reduce equation (1) to 6 unknowns since

$$a_1 = a_2, \theta'_{10} = \theta'_{20}, \theta'''_{10} = \theta'''_{20} = 0. \text{ Hence}$$

$$(5) \lambda = K_{10} e^{-\delta p} + 1 (\theta_{10} + \theta' p) + K_{20} e^{-\delta p} + 1 (\theta_{20} - \theta' p)$$

If, however, the model has asymmetry then a third component must be added to yield: (10, 12)

$$(6) \lambda = (1) + K_3 e^{-\delta p} \int \theta'_3 d\phi$$

The fitting equations as originally derived (3, 11, 12) and as usually utilised, are a perturbation on the constant coefficient solution of the differential equation. This perturbation term, ϵ_1 , is approximated by retaining a term involving the spin as a major factor i.e.: (14)

$$(7) \epsilon_1 = \frac{\bar{m}}{H^2} \frac{[H + 2(T - H - \bar{B})]}{H^2 + 4\bar{m}^2 (2T - H - \bar{B})^2}$$

without detail: the \bar{m}^2 term involves the moment coefficient and the spin, H the damping moment coefficients, T the Magnus moment coefficient and \bar{B} is a rate of change of spin term.

Actually, in programs involving models with essentially zero spin, values are obtained for the perturbation and the rate of change of the rate term, θ'_3 , which seem significant and do not appear chargeable to the effects of spin. The most logical reason remaining is variation of coefficients with Mach number. The actual process of the perturbation does not specify what the variations are, but the term involving the spin is evaluated as the major one for spinning shell. (11, 14) A reconsideration of the perturbation terms, assuming the spin terms are negligible, indicates that the rate of change of the moment coefficient with Mach number is probably the major remaining term. Practically, this term could be of significant size only in the transonic region--but obtaining data in this region is one of the forte's of free flight range testing. The total perturbation term (for spin = 0) is

¹ Appendix B

of the form¹

$$(7a) \frac{\xi}{2} = \frac{1}{L} \left\{ \frac{-M - \frac{H^2}{4} - \frac{H'}{2}}{\left\{ -M - \frac{H^2}{4} - \frac{H'}{2} \right\}} \right\}' + \frac{\frac{1}{L} \left\{ \begin{matrix} M' \\ H' \end{matrix} \right\}}{1 + \frac{H}{2M}}$$

of which the major terms would seem to be

$$\frac{\xi}{2} \approx \frac{1}{L} \left\{ \frac{\frac{c'_M}{c} / \frac{c'_M}{c}}{1 + \frac{1}{2} k_2^2 - \frac{d}{c} c_L - \frac{d}{c} c_D - \frac{dk_2^{-2}}{2d} (c_{Mq} + c_{Ma})} \right\}$$

from the data of the present program the coefficient terms in the denominator are negligible with respect to 1 and hence

$$(8) \frac{\xi}{2} \approx \frac{1}{L} \left[\frac{c'_M}{c} / \frac{c'_M}{c} \right]$$

Considering that rate of change of c_{M_a} is the primary factor, then in terms of the β_j it follows that

$$k_2^{-2} \frac{\partial S_0}{\partial H} \left\{ \frac{c'_M}{c} \right\}' = \beta_1' \beta_2'' + \beta_2' \beta_1''$$

$$I = k_2^{-2} \frac{\partial S_0}{\partial H} c_{M_a}$$

$$H = \frac{\partial S_0}{\partial H} \left[-\frac{d}{c} c_{M_a} - 2\frac{d}{c} c_D - \frac{d}{2d} k_2^{-2} (c_{Mq} + c_{Ma}) \right]$$

$$T = \frac{\partial S_0}{\partial H} \left[-\frac{d}{c} c_{M_a} \frac{d}{c} c_D + \frac{d}{2d} c_{M_a} k_1^{-2} \right]$$

$$n = \bar{v}^2 - 4H - H^2$$

$$\bar{v} = \frac{A}{B} v$$

$$\text{or } (9) \frac{c'_{N_a}}{c'_{N_g}} = \frac{\beta'_1 \beta''_2 + \beta''_1 \beta'_2}{\beta'_1 \beta'_2}$$

and also from the relation of the rates $\dot{\beta}_1 + \dot{\beta}_2 = 0$ (zero spin)

$$\text{so } \beta''_1 + \beta''_2 = 0$$

$$\text{or } \beta'_1 = -\beta'_2, \quad \beta''_1 = -\beta''_2$$

$$\text{let } \beta'_1 = \beta', \quad \beta''_1 = \beta''$$

then (10) becomes

$$\frac{c'_{N_a}}{c'_{N_g}} = \frac{\beta' \beta'' + \beta'' \beta'}{(\beta')} \cdot \frac{2\beta''}{\beta'}$$

and hence c'_{N_a} can be evaluated.

Swerving Motion

The equation fitted to the observations of the missile's motion transverse to its basic trajectory is of the following form when asymmetry is considered:

$$(11) \frac{x + iy}{d} + \frac{iy_g}{d} + \frac{x_g + iy_g}{d} = \frac{s_0}{d} + \frac{s_0}{d} p +$$

$$+ \int_0^P \frac{p s_0}{2m} \left(\left(\frac{d}{c} \right) c_{N_a} - \frac{ivb}{c} c_{N_{pq}} \right) \lambda d\phi d\psi + \int_0^P \frac{p s_0}{2m} \left((c_{N_g} + c_{N_a}) + iv(c_{N_{pq}} - c_{N_g}) \right)$$

$$(\lambda - \lambda_y) \Phi$$

$$- \left(\frac{d}{c} \right) \frac{p s_0}{2m} c_{N_a} \lambda \int_0^P \int_0^P e^{i \int \beta'_3 d\phi} \Phi d\phi$$

The last term is omitted for symmetric reductions, and reductions with the terms involving the spin set equal to zero are also utilized. Once the yaw fit has been established the integral may be evaluated by several means as discussed in Ref. 12. The subscript "g" terms are gravity corrections, the "a" subscript terms are Coriolis corrections.

Center of Mass Transformation

In order to determine the force coefficients from moment data or to apply the data pertaining to one center of mass position to another there are relations between the coefficients for the cases. (3, 10, 13) Asterisks represent the values of a given coefficient at a new c.g. position in terms of those at another position separated by a distance \bar{q} (in calibers, positive if the motion from the old to the new is noseward)

$$(12) \quad C_{N_c}^* = C_{N_c}$$

$$(C_{N_q} + C_{N_a})^* = (C_{N_q} + C_{N_a}) + 2 \bar{q} C_{N_a}$$

$$C_{M_a}^* = C_{M_a} + \bar{q} C_{N_a} \left(\frac{d}{c}\right)$$

$$(C_{M_q} + C_{M_a})^* = (C_{M_q} + C_{M_a}) + \bar{q} \left[(C_{N_q} + C_{N_a}) + 2C_{N_a} \right] - 2\bar{q}^2 C_{N_a}$$

Modified damping relation

$$\left[(C_{M_q} + C_{M_a})^* - 2 \bar{q} (C_{M_a})^* \right] = (C_{M_q} + C_{M_a}) + \bar{q} (C_{N_q} + C_{N_a}).$$

APPENDIX B

One of the more annoying points in programs of this nature is the persistent appearance of roll and trim that indicate that the model is not perfect. The question always arises as to whether it is sufficient to apply the simpler symmetric reductions or whether it is necessary to apply the more complicated techniques of reduction. In order to evaluate this, for models of the present program, a series of reductions were run on some rounds and on some computed trajectories and yawing motions.

Effect of Slow Rolling

Table V gives a comparison of two types of symmetric reductions on two actual rounds and three computed motions. The six-unknown reduction postulates no spin while the ten-unknown permits spin and variation of spin. For the two actual rounds there was little or no significant difference between the two reductions. The spin level involved was small ($1/2$ deg per foot). In the case of the computed motions an actual effect of about 1% error in the damping was incurred by applying the six-unknown reduction up to a roll rate of $1^{\circ}/ft$. (Roll rates on the order of two degrees per foot had previously caused trouble so that it was a question of what lower values would do.)

Effect of Trim

In order to evaluate the effect of various trims on the results from symmetric reductions of the yawing and swerving motions, reductions of motions with and without known trim were tried. A yawing motion was computed from the symmetric equation and reduced and a similar motion with trim was computed and reduced ignoring the trim. A swerving motion was computed from the symmetric equations for this motion and for three different trim levels and treated by symmetric reductions.

Table VI shows the effect of various levels of asymmetry on the damping moment determination and on the lift and damping force determination from the swerve. Considering the yawing motion, trim angles which might be just visible in the data (.0025 radians) produced an error in the damping moment determination of about 4%. A trim of .005 radians, which should be quite evident, produced about a 13% error. The yaw moment coefficient was not seriously affected. The case of the swerving motion is much more sensitive. A trim angle of .002 radians yielded a statistical error of 10% for the lift coefficient from the fit (the actual difference between input G_L and computed was of the order of 1%

but this might be fortuitous). The same trim gave an error for the damping force coefficients of 35% (actual difference 11%). However, a change of about 2% occurred for trims as low as .0005 radians. Hence it appears that errors in the lift determination of up to 5% and in the damping force up to 10% might result from asymmetries that are not immediately evident in the raw data and might even be obscured in a final fit. Visible trims can produce marked errors in the lift and damping force determination from the swerve and may introduce significant errors in the damping moment determination.

APPENDIX C

TABLE I

Round No.	Mach No.	Mass gm	A in ²	B in ²	c.g. in from base
2588	1.802	147.65	13.47	551.46	3.112
2589	1.817	147.73	13.52	552.53	3.114
2590	1.903	147.68	13.51	552.06	3.112
2595	1.784	147.77	13.71	552.73	3.109
2596	1.814	255.95	26.69	864.84	2.252
2598	1.798	255.95	25.88	859.61	2.258
2599	1.788	254.65	27.02	864.46	2.250
2591	1.801	255.39	19.80	896.31	4.002
2593	1.733	249.48	19.87	896.67	3.999
2594	1.745	249.60	19.94	897.99	4.001
3246	1.398	227.02	20.02	813.57	3.045
3247	1.264	227.15	19.78	811.52	3.056
3248	1.077	228.18	20.43	816.14	3.035
3249	2.050	227.14	19.99	813.72	3.051
3252	1.011	227.38	20.04	811.11	3.044
3253	1.047	227.57	28.18	812.44	3.043
3254	1.506	313.82	28.60	1053.2	2.592
3255	2.032	313.11	28.90	1054.5	2.588
3256	1.993	312.03	28.45	1049.2	2.588
3257	1.390	312.46	28.33	1050.3	2.598
3258	1.139	311.95	28.09	1050.3	2.599
3259	1.084	313.00	28.49	1050.8	2.590
3260	1.017	313.38	28.49	1059.2	2.597
3261	0.975	311.41	28.21	1045.0	2.595
3262	1.044	312.38	28.41	1047.7	2.590
3263	2.123	311.56	28.28	1010.8	2.595
3264	2.468	227.26	19.91	819.02	3.076

TABLE IV

<u>Round No.</u>	<u>M</u>	<u>Ave Yaw°</u>	<u>Method</u>	<u>Remarks</u>
2588	1.80	0.7	Shear Pin	
89	1.83	0.9	"	
90	1.80	0.3	"	
95	1.78	0.8	"	
96	1.81	1.2	"	
98	1.80	2.4	"	
99	1.79	1.2	"	
91	1.80	0.5	"	
93	1.73	7.4	"	
94	1.74	6.0	"	
3246	1.40	4.2	Electro- Magnetic Yaw Inducer	
47	1.26	2.5		
48	1.08	0.5		
49	2.05	2.3		
52	1.01	0.5		
53	1.05	0.6		
54	1.51	1.9		
55	2.03	0	"	Model Magnet de- magnetized
56	1.99	2.6	"	
57	1.39	0.7	"	
58	1.14	2.3	"	
59	1.08	0	"	
60	1.02	0	"	
61	0.98	4.3	"	
62	1.04	0.3	"	
63	2.42	1.7	"	
64	2.47	0.5	"	

TABLE III
REDUCTION VALUES

Round No.	Mach No.	$\frac{g^2}{(\text{deg})^2}$	C_D	C_{N_a} (per rad)	$-C_{H_d}$ (per rad)	$- (C_{H_d} + C_{H_d^0})$ C_{H_d}	$(C_{H_d} + C_{H_d^0})$ C_{H_d}
2588	1.802	0.4	0.616	8 (25%)	22.61 (0.7%)	266 (11%)	
89	1.827	0.7	0.614	11 (16%)	21.95 (0.6%)	340 (8%)	
90	1.803	0.1	0.614				
95	1.784	0.6	0.624		22.27 (0.6%)	238 (11%)	
96	1.814	1.5	0.629	15 (11%)	9.12 (0.6%)	163 (11%)	
98	1.798	5.6	0.621	15 (11%)	9.81 (0.4%)	21.6 (8%)	
99	1.788	1.5	0.662	15 (19%)	9.56 (1.0%)	178 (22%)	
91	1.801	0.2	0.604	5 (9%)	36.58 (0.6%)	548 (8%)	
93	1.733	53.4	0.873	13 (25%)	39.69 (0.4%)	466 (7%)	
94	1.745	36.2	0.777	12.6(3%)	39.29 (0.05%)	518 (7%)	
3246	1.398	17.8	0.789	16.3(3.3%)	34.9 (0.2%)	326 (4%)	
47	1.264	6.2	0.753	16.7(4.4%)	41.1 (0.2%)	349 (3%)	- 108 (149%)
48	1.077	0.2	0.895	19.0(19.5%)	40.0 (0.9%)	173 (11%)	
49	2.050	5.0	0.526	10.3(1.3%)	16.8 (0.1%)	304 (3%)	
52	1.011	0.2	0.889	9.3(56.5%)	37.7 (0.0%)	541 (%)	
53	1.047	0.3	0.883	15.7(22.3%)	38.0 (%)	283 (%)	- 289 (240%)
54	1.506	3.7	0.710	10.2(20.2%)	21.8 (0.3%)	333 (8%)	
55	2.032		0.568				
56	1.993	6.6	0.584	11.2(1.4%)	10.8 (0.0%)	165 (%)	
57	1.390	0.5	0.706		25.9 (%)		
58	1.139	5.4	0.850	17.9(4.1%)	27.8 (0.0%)	191 (%)	
59	1.084		0.884		26.9 (0.0%)	138 (%)	
60	1.017	0	0.900		27.8 (5.1%)	177 (35%)	
61	0.975	18.4	0.893	19.6(5.0%)	32.6 (1.3%)	-91 (135%)	
62	1.014	0.1	0.905	31.9(27.4%)	30.1 (1.7%)	170 (11%)	
63	2.023	2.9	0.478	9.7(1.3%)	6.5 (0.6%)		
64	2.468	0.2	0.449		11.7		

TABLE IV
VARIATION OF AERODYNAMIC PROPERTIES AND OBSERVABLE PHENOMENA

Mach No.	Phenomena			
	1.04	1.15	1.4	2.4
Property	Mach Number			
C_D	Maximum	Approximately end of region of increasing slope with decreasing M	Region of rapid increase with decreasing M	
$\cdot C_{D_0}$	Near local minimum	Near minimum	Approximately point of maximum decrease with decreasing M	
C_P	Possibly maximum aft position	local maximum forward position	Local maximum aft position	Region where rate of forward motion with increase of M decreases
$\cdot C_{P_0}$	Local maximum	Minimum		
$\cdot (C_{P_0} + C_{H_0})$	Maximum		Local minimum	Local maximum (?)
$\cdot (C_{B_0} + C_{H_0})$	Near minimum		Maximum	Local minimum (?)

TABLE V
COMPARISON OF REDUCTION TYPES
ZERO TRIM

Case	$\frac{-C_{H_0}}{C_S} \cdot \left[C_L = C_D + \frac{1}{2} k^2 (C_{M_q} + C_{M_0}) \right]$		Reduction Type
Computed: 0°/ft Spin	12.27 0%	7.32 0%	6 unknowns
Computed: 0.5°/ft Spin	12.21 1.0 %	7.41 1.3 %	6 unknowns
Computed: 1.0°/ft Spin	12.21 1.1 %	7.40 1.3 %	6 unknowns
Round 2594 (Spin ~1/2 °/ft)	39.29 0.05%	55.21 0.6 %	6 unknowns
	39.22 0.08%	55.95 0.7%	10 unknowns
Round 2598 (Spin ~1/2 °/ft)	9.80 0.41%	30.81 4.9 %	6 unknowns
	10.01 0.76%	31.58 8.0	10 unknowns

TABLE VI

EFFECT OF TRIM ON COEFFICIENTS OBTAINED FROM SYMMETRIC YAW AND SWERVE REDUCTIONS

YAW REDUCTION VALUES

Case	$-C_{M_a}$	$-C_{L_a} - C_D + 1/2 k^2 (C_{H_q} + C_{H_a})$
1. Computed yawing motion with zero trim	20.04 0	25.94 0
2. Computed yawing motion with .0025 rad trim	20.06 0.3	26.96 3.6
3. Yawing motion of round 2598	9.80 0.4	30.9 4.9
4. Yawing motion of round 2598 + .005 rad trim	9.93 1.2	37.0 12.7

SWERVE REDUCTION VALUES

	$-C_{L_a}$	$-(C_{H_q} + C_{H_a})$
Computed swerving motion with zero trim	11.46 0	122.8 0
Computed with .0005 trim	11.48 2.4	150.7 8
Computed with .001 trim	11.51 4.8	113.6 16
Computed with .002 trim	11.53 9.7	131.9 35

DISTRIBUTION LIST

<u>No. of Copies</u>	<u>Organization</u>	<u>No. of Copies</u>	<u>Organization</u>
	Chief of Ordnance Department of the Army Washington 25, D.C. Attn: CRDTB - Sec 1 Soc	2	Commander Naval Ordnance Test Station China Lake, California Attn: Tech Library
3	Chief, Bureau of Ordnance Department of the Navy Washington 25, D.C. Attn: Reg	1	Commander Arnold Engineering Development Center Tullahoma, Tennessee Attn: Deputy Chief of Staff, R&D
2	Commander Naval Proving Ground Dahlgren, Virginia	1	Commander Air Research and Development Command P.O. Box 1395 Baltimore 3, Maryland Attn: Deputy for Develop- ment
2	Commander Naval Ordnance Laboratory White Oak Silver Spring, Md. Attn: Mr. Nestingen Mr. May	5	Director Armed Services Tech Information Agency Documents Service Center Knott Building Dayton 2, Ohio Attn: DSC-SA
1	Superintendent Naval Postgraduate School Monterey, California	4	ASTIA Reference Center Tech Information Division Library of Congress Washington 25, D.C.
2	Commander Naval Air Missile Test Center Point Mugu, California	3	Director National Advisory Committee for Aeronautics 1512 H Street, N.W. Washington 25, D.C.
1	Commanding Officer and Director David W. Taylor Model Basin Washington 7, D.C. Attn: Aerodynamics Lab.	2	Director National Advisory Committee for Aeronautics Ames Laboratory Moffett Field, California Attn: Dr. A.C. Charters Mr. H.J. Allen
1	Commander Naval Air Development Center Johnsville, Perma.		

DISTRIBUTION LIST

<u>No. of Copies</u>	<u>Organization</u>	<u>No. of Copies</u>	<u>Organization</u>
3	National Advisory Committee for Aeronautics Langley Memorial Aeronautical Lab. Langley Field, Virginia Attn: Mr. J. Bird Mr. C. E. Brown Dr. Adolf Busemann	2	Director, JPL Ordnance Corps Installation Department of the Army 1800 Oak Grove Drive Pasadena 2, California Attn: Mr. Irl E. Newlan, Reports Group
1	National Advisory Committee for Aeronautics Lewis Flight Propulsion Laboratory Cleveland Airport Cleveland, Ohio Attn: F. K. Moore	1	Director, Operations Research Office 7100 Connecticut Avenue Chevy Chase, Maryland Washington 15, D.C.
1	Director National Bureau of Standards Connecticut Avenue & Van Ness Street, N.W. Washington 25, D.C.	2	Armour Research Foundation 35 W. 33rd Street Chicago 16, Illinois Attn: Mr. W. Casier Dr. A. Wundheiler
1	Commanding General Redstone Arsenal Southville, Alabama Attn: Tech Library	1	Aerophysics Development Corp. P.O. Box 657 Pacific Palisades, Calif. Attn: Mr. William Bollay
3	Commanding Officer Picatinny Arsenal Dover, New Jersey Attn: Samuel Feltman Ammunition Laboratories	1	California Institute of Technology Norman Bridge Laboratory of Physics Pasadena, California Attn: Dr. Leverett Davis, Jr.
1	Commanding General Frankford Arsenal Philadelphia 37, Penna. Attn: Reports Group	1	Consolidated Vultee Aircraft Corp. Ordnance Aerophysics Lab. Daingerfield, Texas Attn: Mr. J.E. Arnold
1	Commanding Officer Chemical Corps Chemical & Radiological Laboratory Army Chemical Center, Md.	1	Cornell Aeronautical Laboratory, Inc. 4455 Genesee Street Buffalo, New York Attn: Miss Edna T. Evans, Librarian

DISTRIBUTION LIST

<u>No. of Copies</u>	<u>Organization</u>	<u>No. of Copies</u>	<u>Organization</u>
1	California Institute of Technology Guggenheim Aeronautical Pasadena, California Attn: Professor H.W. Liepmann	1	Dr. A. L. Buckett Hughes Aircraft Company Florence Avenue at Teal Street Culver City, California
1	General Electric Co. Project HERMES Schenectady, New York Attn: Mr. J.C. Hoffman	1	Professor George Carrier Division of Applied Sciences Harvard University Cambridge 38, Mass.
2	Sandia Corporation Sandia Base P.O. Box 5800 Albuquerque, New Mexico Attn: Mr. Wynne K. Cox	1	Professor Francis H. Clauser Department of Aeronautics Johns Hopkins University Baltimore 18, Maryland
1	University of Michigan Willow Run Research Center Willow Run Airport Ipsilanti, Michigan Attn: Mr. J. E. Corey		
1	United Aircraft Corp. Research Department East Hartford 8, Connecticut Attn: Mr. C. H. King		
1	University of Southern California Engineering Center Los Angeles 7, California Attn: Mr. H. R. Saffell, Director		
1	Professor Clark B. Millikan Guggenheim Aeronautical Laboratory California Institute of Technology Pasadena 11, California		